Bidimensional Spectroelectrochemistry Applied to the Electrosynthesis and Characterization of Conducting Polymers: Study of Poly[4,4′-bis(butylthio)-2,2′-bithiophene]

by **Virginia Ruiz**, **Álvaro Colina**, **Aránzazu Heras**, and **Jesús López-Palacios***

Departamento de Química, Universidad de Burgos, Pza. Misael Bañuelos, s/n, E-09001 Burgos

and **Renato Seeber**

Dipartimento di Chimica, Università di Modena, Via G. Campi, 183, I-41100 Modena

Dedicated to Prof. *André M. Braun* on the occasion of his 60th birthday

The electropolymerization mechanism of 4,4′-bis(butylthio)-2,2′-bithiophene (**1**) was studied by means of bidimensional spectroelectrochemistry. Simultaneous electrochemical and spectroscopic signals were analyzed with the aim of obtaining information about the role of the low-molecular-weight oligomers in the polymerization process. Experiments in electrochemical cells with finite (thin layer) and semi-infinite diffusion geometries were carried out to elucidate the role the oligomeric species play, both in the nucleation step and in the subsequent growth of the polymer deposited onto the electrode surface.

1. Introduction. – New organic conducting polymeric materials have experienced very rapid development in the last two decades. In particular, many different conducting polymers with a polythiophene backbone have been synthesized and characterized, and effective applications in various fields, such as primary and secondary batteries, electronic and electro-optical devices, and chemical sensors have been proposed [1–5]. In particular, a large number of functionalized polythiophenes have been proposed for possible applications in chemical sensors and as electrode modifiers in amperometric sensor devices [6–10].

Poly(β-substituted thiophene)s can be synthesized by either chemical or electrochemical methods starting from the corresponding β-substituted thiophenes or β,β'-disubstituted bithiophenes. Low values for the oxidation potential and regioregularity of the resulting polymers are among the factors that encouraged hard work on the synthesis and study of the properties of new poly(β,β'-disubstituted bithiophene)s. The regiochemistry of the resulting polymer strongly affects the relevant physical properties: as an example, conductivity is much higher in regioregular head-to-tail than in regiorandom polythiophenes. Furthermore, poly[4,4′-bis(alkylthio)-2,2′-bithiophene]s can be easily electrogenerated [11–14] and proved to lead to quite stable electrode coatings, even over relatively long times and under polarization conditions [15–17], thus allowing the attainment of reliable and repeatable voltammetric responses.

Together with detailed studies on the physical, chemical, electronic, and electrochemical properties of polythiophenes [12][13][15][18][19], a number of studies have been carried out on the mechanism of the processes taking place at the electrode/

solution interface during electrogeneration of these polymers [20–27]. In the present paper, a novel experimental technique is presented and proposed to study processes simultaneously taking place in the solution and on the surface during electropolymerization.

A general scheme has been proposed for anodic electropolymerization of heterocycles [6][28]. The first electrochemical step (E) consists of the oxidation of the monomer to a radical cation. The second step involves the coupling of two radical cations to produce a dihydro dimer dication, which leads to the dimer by loss of two protons with consequent re-aromatization, which is the driving force for this chemical step (C). The dimer, at the applied potential, is oxidized in its turn to the corresponding radical cation and undergoes a further coupling with another radical cation. Electropolymerization proceeds then through successive electrochemical and chemical steps according to a general $E(CE)_n$ scheme, until the oligomer becomes insoluble and precipitates onto the electrode surface.

However, several steps of this process are not fully understood yet and are still the subject of controversial interpretations; this is the case regarding the exact role of oligomers in the initial deposition step and in the subsequent growth of the polymer chains [29]. Using UV/VIS transmission spectroscopy and ellipsometry, *Hillman et al.* studied the electropolymerization of thiophene [30][31] and bithiophene [32] and concluded that the formation of oligomers in solution precedes the polymer deposition and that the fraction of soluble oligomers escaping into the solution bulk is very low. *Tanaka* and co-workers [33] could detect oxidized soluble oligomers during the electropolymerization of thiophene by using a Pt rotating-ring-disk electrode system.

The adsorption of the thiophene monomer on the electrode surface has also been proposed as the first step [34]. This observation is difficult to reconcile with the hypothesis of the formation of oligomers in the solution, since it is not easy to imagine the reason why the monomer, once adsorbed, leaves the electrode surface to form oligomers inside the solution. *John* and *Wallace* [35] postulated that the growth of electropolymerized polypyrrole onto Pt microelectrodes is largely the result of precipitation of oligomeric or polymeric species from the solution rather than the sequential addition of pyrrole monomers to the chain ends of the deposited polymer. On the other hand, *Casalbore-Miceli et al.* [36] suggested the occurrence of two steps in the electropolymerization of substituted bithiophenes onto ITO electrodes: an initial induction step leading to electrode covering and a successive one leading to film growing on the polymer-coated electrode. In the former step, the coupling between radical cations leads to the formation of oligomers that can *i*) be oxidized further, or *ii*) precipitate onto the electrode, or *iii*) diffuse into the solution bulk as soluble products that do not participate to the polymer formation. These authors postulate that, after this initial covering stage, production of soluble species decreases and, therefore, the mechanism of the polymer growth is different in the two steps. In particular, they suggest that polymerization on a polymer-coated electrode occurs probably by direct reaction between soluble radical cations and the polymer chains of the already formed deposit on the electrode.

Smie et al. [11] studied the electropolymerization of 4,4′-bis(methylthio)-2,2′-bithiophene. They suggested that the electropolymerization mechanism of donor-substituted thiophenes does not involve a chain-propagation process through

successive coupling steps of the starting radical cations to the growing chain, as it was postulated previously [37]. By contrast, they concluded that oligomerization of these compounds in solution preferably occurs *via* consecutive dimerization steps leading from a dimer to the tetramer and then to an octamer, and so on. More recently, identical phenomena have been observed by *Heinze et al.* in the case of alkoxy-substituted thiophenes [26].

Schindler and co-workers [38] used UV/VIS absorption spectroscopy to identify the species present in the diffusion layer during electropolymerization of thiophene at Pt electrodes. The absorbing species were identified as neutral, radical-cationic, and dicationic oligomers of thiophene. The authors carried out separately two types of experiments, using a Pt-mesh electrode and a long-path cell. In both cases, contributions due to absorbance resulting from the deposited film were excluded. Therefore, measurements in both experimental arrangements supplied information only about species present in the diffusion layer and inside the solution.

In the present paper, both types of possible optical measurements, *i.e.*, normal and parallel to the electrode surface, were performed simultaneously during electropolymerization of 4,4′-bis(butylthio)-2,2′-bithiophene (**1**). Spectroscopic information along both directions could be obtained with a spectroelectrochemical cell designed and constructed in our laboratory. In this way, it was possible to monitor the absorbance contribution due to the electrodeposited polymer (normal-beam arrangement) and that due to the species in solution (parallel-beam arrangement) at the same time during electropolymerization. This simultaneous observation of the phenomena taking place in solution and at the surface allowed us to detect soluble oligomeric intermediates and to establish their role in the different stages of the polymer growth.

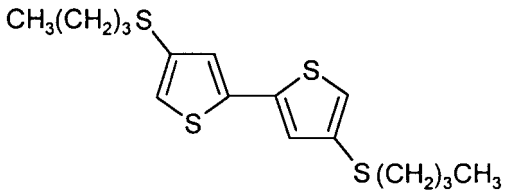

1

2. Methodology. – Bidimensional spectroelectrochemistry [39] is a recent technique that allows simultaneous acquisition of spectra in both normal and parallel directions to the surface of a plane electrode to which a potential is imposed (*Fig. 1*). The absorbance in the parallel direction, A_P, contains information about the processes occurring in the solution layer close to the electrode (diffusion, homogeneous chemical reactions), but is insensitive to the phenomena occurring at the electrode surface (polymer deposit formation and growth). Absorbance in parallel direction is given by *Eqn. 1*, where ε is the molar absorptivity of the absorbing species at a C_{sol} concentration in the solution, and l is the optical path length. *Eqn. 1* can be directly applied only when C_{sol} can be considered constant at any distance from the electrode within the extremes of the light-beam section. If this condition is not fulfilled, the absorbance in every parallel-to-electrode infinitesimal-thickness layer is different, and the measured absorbance [40] is a function of the distance x from the electrode, as defined in

Eqn. 2, where ω is the diffusion-layer thickness, which is actually lower than the diameter of the beam section.

$$A_P = \varepsilon\, l\, C_{sol} \tag{1}$$

$$A_P = \log\left(\frac{\omega}{\int_0^{\omega} 10^{-\varepsilon l c(x)} dx}\right) \tag{2}$$

On the other hand, the absorbance measured perpendicularly to the electrode surface, A_N, is given by *Eqn. 3*, where ε_s is the absorptivity per unit area, Γ is the amount of absorber deposited onto a unit area, ω is, also in this case, equal to the path length, and C_{disol} represents the average concentration of the parallel-to-electrode layers (see *Eqn. 4*). Obviously, A_N includes the absorbance of both soluble and electrodeposited species.

$$A_N = \varepsilon_s \Gamma + \varepsilon \omega C_{disol} \tag{3}$$

$$C_{disol} = \frac{1}{\omega} \int_0^{\omega} C(x) dx \tag{4}$$

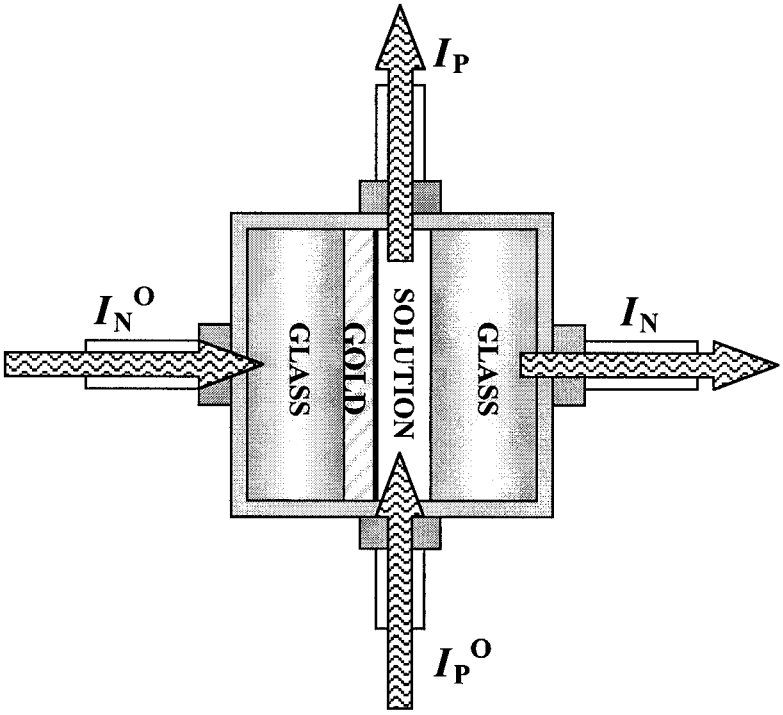

Fig. 1. *Top view of the cell used for bidimensional spectroelectrochemistry.* Only the Au working electrode is represented. I_P^o, incident parallel-beam intensity; I_P, beam intensity exiting the cell in the parallel-beam arrangement; I_N^o, incident normal-beam intensity; I_N, beam intensity exiting the cell in the normal-beam arrangement.

Therefore, in principle, bidimensional spectroelectrochemistry is a suitable technique for studying processes like electropolymerization, in which different reactions occur at the electrode surface and inside the solution layer very close to the electrode. The spectroelectrochemical measurements are profitably carried out in two types of cells, different from each other as to geometry of diffusion: a cell where semi-infinite diffusion is operative allows the electroactive species to reach the electrode surface from a relatively far point inside the solution. A flat concentration profile of the electroactive species cannot be obtained in this type of cell, because the bulk concentration remains unchanged during the short time of the electrolytic process. On the other hand, a thin-layer cell forces the sample into a diffusion layer of finite thickness, allowing a flat concentration profile to be attained easily. This latter kind of cell has been chosen for most of our experiments for two different reasons: *a*) absorbance changes in the parallel direction are higher, thanks to the constraint imposed on the diffusion layer by the geometry and the consequently higher change in concentration of the absorbing species during the electrolytic reaction; *b*) flat concentration profiles guarantee homogeneity of the solution and correct applicability of *Eqns. 1* and *3*. Under such conditions, the absorbance of the polymer on the electrode can be accurately obtained from the difference between A_N and A_P. From a quantitative point of view, the absorbance due to the deposited polymer alone can be obtained from the measure obtained in the normal-beam arrangement, when corrected by subtracting the value of the weighted absorbance in the parallel-beam arrangement according to *Eqn. 5*, where A_N^C is the corrected normal-beam absorbance.

$$A_N^C = A_N - A_P \cdot \frac{\omega}{l} \tag{5}$$

3. Results and Discussion. – 3.1. *Electrosynthesis of Poly[4,4′-bis(butylthio)-2,2′-bithiophene]*. Electropolymerization was performed under potentiodynamic conditions, with solutions of various dimer concentrations and allowing the voltammetric scan to reach different positive potentials. As an example, *Fig. 2* shows the current-potential curves recorded in 20 subsequent potential cycles from 0.00 to +1.16 V, in a solution at $2 \cdot 10^{-3}$ M dimer concentration. The potential scan rate was 0.04 V s^{-1}, and the diffusion space was limited to 150 μm by means of suitable spacers.

As a first observation, the current intensity relative to polaron formation inside the polymer deposit increases at every cycle, which means that the thickness of the polymer onto the electrode progressively increases, which, in its turn, implies that the initial dimer in the diffusion space is not totally consumed during the experiment. *Fig. 2* shows that electro-oxidation of the dimer (I_{an}) takes place around +1.0 V. As the polymer grows on the electrode surface, an oxidation peak appears around +0.6 V, accounting for the formation of polarons inside the polymer (peak II_{an}). In the backward sweep, two reduction waves can be clearly detected, one at +0.4 V (peak II_{cat}), corresponding to the reduction step of peak II_{an}, and another one at *ca.* +0.8 V (III_{cat}) that, taking into account the irreversibility [11] of the dimer electro-oxidation (I_{an}), can only be explained as the reduction stage corresponding to the bipolaron formation (III_{an}), ill-defined in the anodic scan.

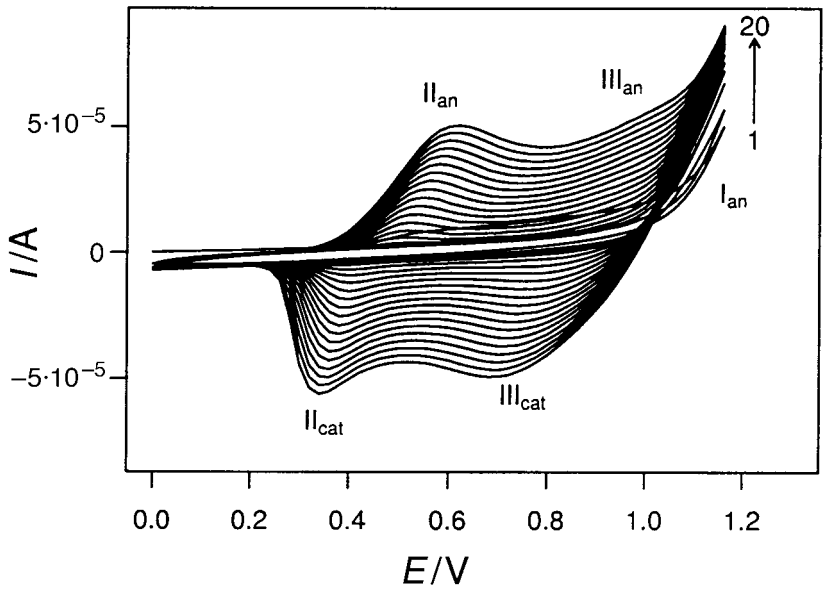

Fig. 2. *Cyclic voltammogram obtained during the electropolymerization of 4,4′-bis(butylthio)-2,2′-bithiophene* (**1**). Concentration of dimer, $2\cdot10^{-3}$ M; concentration of $(Bu_4N)PF_6$, 0.1M; number of cycles, 20; potential scan rate; 0.04 $V\cdot s^{-1}$; potential range, from 0.00 to +1.16 V; diffusion space, 150 μm; thin-layer cell.

In these tests, spectra in both normal and parallel configuration were recorded concomitantly to the measurement of the current. *Fig. 3* shows the spectra recorded during a potential cycle at the two extreme potential values, *i.e.*, at 0.00 and +1.16 V, respectively. In the normal configuration, *i.e.*, when the optical path is perpendicular to the electrode surface, the neutral forms of the oligomeric and polymeric species (spectrum at 0.00 V) show a maximum absorbance at 564 nm; under the same conditions, the corresponding oxidized forms (spectrum at +1.16 V) exhibit a very wide absorption band with a poorly defined maximum around 750 nm. The parallel arrangement gives dramatically different spectra: at both polarization potentials, the maximum absorbance is around 378 nm. These results suggest that different species are 'observed' in either configuration. In particular, the spectra obtained in the parallel configuration should arise from soluble oligomers generated during the electropolymerization.

Fig. 4 shows the absorbance values in parallel and normal configurations at 400 and 564 nm plotted against the applied potential during 20 subsequent voltammetric cycles. The 400-nm wavelength, which is very close to the value of the maximum absorbance in the parallel configuration, was chosen to display the results because at this wavelength, both oxidized and neutral oligomeric forms exhibit the same absorptivity; thus, the absorbances measured in the parallel and normal arrangement are related to the overall amount of soluble and of electrodeposited species, respectively. To clarify the display, only representative cycles are plotted in *Fig. 4,a*. As we can see therein, the concentration of soluble species increases during the first four cycles, assuming a practically constant value in the subsequent sweeps. Beside this, the plot of the

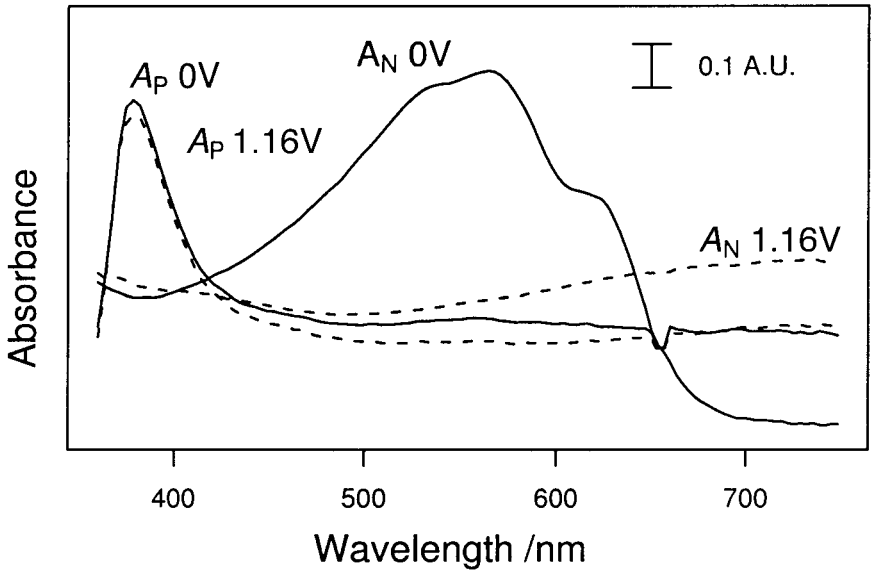

Fig. 3. *Absorbance spectra in the normal* (A_N) *and parallel-beam* (A_P) *configurations at 0.00 V* (–) *and +1.16 V* (––) *corresponding to a potential cycle of the experience shown in* Fig. 2

corrected normal absorbance, A_N^C, at the same wavelength shows (*Fig. 4,b*) that the polymer film grows at a constant rate at any stages of the process, except for the first two cycles, in which an absorbance value near zero implies that no significant amount of polymer has formed.

Fig. 4,c reports the evolution of the parallel absorbance at 564 nm with the potential, in the same experiment. As indicated above, this wavelength corresponds to the absorbance maximum of the neutral form of the polymer. The evolution of the absorbance with the potential exhibits a trend similar to that displayed in *Fig. 4,a:* in subsequent cycles, it assumes increasing values during the first four cycles, crosses a maximum, and finally decreases to describe absorbance *vs.* potential traces well overlapping each other. On the contrary, the absorbance measured in normal configuration (*Fig. 4,d*) continuously increases with the number of cycles, though, as expected, the values at the most positive potentials are quite low. This behavior is in agreement with the assignment of the corrected normal signal to the growing polymer and of the parallel spectral signal to the oligomers formed during the electropolymerization.

The maximum concentration of soluble oligomers is attained after the first cycles, as is evident from *Figs. 4,a* and *c*, when only small quantities of polymer (nucleation step) form (see *Figs. 4,b* and *d*). From the third cycle onwards, generation of a significant amount of polymer can be observed on the electrode surface. The A_N^C value at 400 nm remains constant during every cycle over the entire potential range, since both oxidized and neutral forms of the polymer exhibit equal absorptivity at this wavelength; at 564 nm (*Fig. 4,d*), it is possible to differentiate between oxidized and neutral forms of

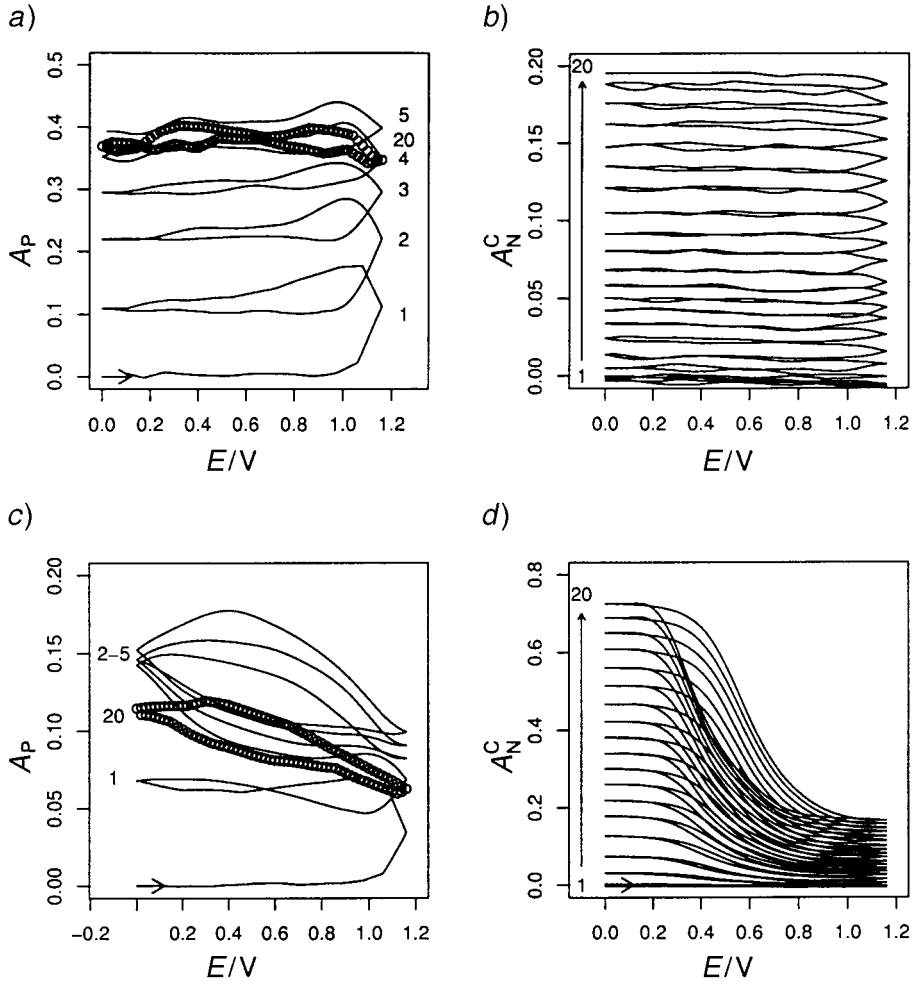

Fig. 4. *Absorbance* vs. *potential in the same test as in* Fig. 2: a) A_P *at 400 nm and* b) A_N^C *at 400 nm*; c) A_P *at 564 nm and* d) A_N^C *at 564 nm*. In *a*) and *c*), the first five cycles are shown by solid line and the last cycle by circles (only some most representative traces are reported in these cases).

the polymer (see *Fig. 3*). The amount of polymer generated in every cycle is constant, leading to increasing absorbance values.

3.2. *Role of the Oligomers.* During the first steps of the polymerization process, some different oligomeric species absorbing at different wavelengths can be detected, as it has been proposed in [38]. *Fig. 4*, *a* shows that the oligomers start being generated around $+1.0$ V during the first five oxidation scans, but only a minor fraction of the species 'disappears' during the subsequent backward scan to give the first nucleation sites on the electrode surface. From the sixth cycle on, a steady-state concentration of oligomers is reached in the diffusion space.

With respect to the absorbance at 564 nm, from *Fig. 4*, *c*, we can assume that it accounts for electrogenerated species, since it decreases during the anodic scans, *i.e.*, when oxidized species arise, and increases during the cathodic scans, when they are neutralized. Also, these plots support the achievement of a steady-state situation after a given number of potential cycles.

According to these results, the electropolymerization can be explained as a sequential process. Soluble oligomers are always present in the diffusion layer, inducing the formation of polymer nuclei at the electrode. However, after nucleation has begun, the role of the oligomers is not so clear. Two different hypotheses were considered: *1*) generation of oligomers takes place only during the first step of the electropolymerization, *i.e.*, before electrode covering, and stops afterwards, the polymer chain growing by addition of monomer units [36]; *2*) the oligomers continue to be generated and play an active role in the polymer growth.

With the aim of finding a reliable explanation to the role of the oligomers, experiments under conditions of semi-infinite diffusion were also carried out (see the description of the spectroelectrochemical cell in the *Exper. Part*). Under this diffusional-geometry condition, if hypothesis *1*) were true, the parallel absorbance close to the electrode surface due to the oligomers would decrease after the appearance of the polymer film, since the oligomers that are not involved in the first formation of polymer should diffuse into the bulk of solution. If hypothesis *2*) were true, A_P should remain unchanged in the proximity of the electrode.

A comparison of the experiments carried out under thin-layer and semi-infinite diffusion conditions is summarized in *Fig. 5*. Only the dimensions of the diffusion space change from one set of experiments to the other, maintaining the rest of experimental conditions unchanged. *Fig. 5* shows the evolution of A_P at 400 nm and 0.00 V polarizing potential *vs.* the number of cycles in both kinds of cells. As we can see, the absorbance of oligomers in the semi-infinite geometry cell does not decrease after the nucleation step. From these plots, we conclude that the first hypothesis must be rejected and that oligomers are continuously generated at the electrode, even after the polymer film forms on the surface. Also, from the constancy of A_P in the semi-infinite diffusion geometry after a given number of cycles, it is clear that, without previous generation of a high enough concentration of intermediate oligomers, the polymerization does not take place, and, from this point of view, the process follows a sequential mechanism. However, when the electrode surface is completely coated by a polymer film, both processes, *i.e.*, oligomer and polymer formation, occur. If the reaction takes place within a finite space, like in a thin-layer cell, the fact that A_P is unchanged implies that the oligomers participate actively in polymer growth. Therefore, there is no reason to suggest a different mechanism for the two polymerization steps, and we discard the hypothesis of deposit growth by addition of oxidized dimeric units to the oxidized polymer chain.

On the basis of the above results, we have to assume that oxidation of dimers leads to radical cations that combine with each other to give tetramers; tetramers are more easily oxidized than the dimers and, once oxidized, they lead to hexamers or octamers, and so on as far as a critical number of units in the chain is reached, leading to formation of a solid-phase precipitate on the electrode (nucleation step). The relatively small size and consequent solubility of some oligomers allows them to diffuse away

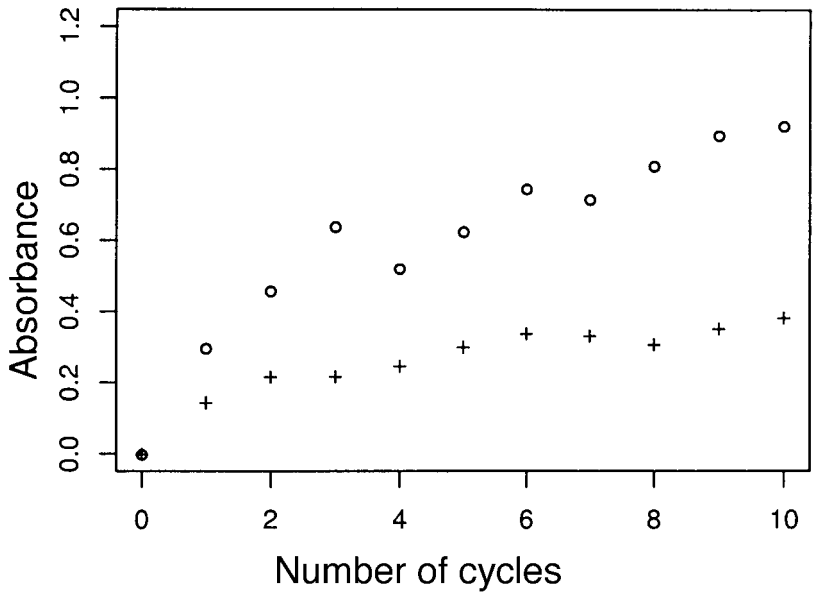

Fig. 5. *Evolution of the parallel absorbance* A_P *at 400 nm measured at 0.00 V under thin-layer* (○) *and semi-infinite* (+) *diffusion conditions* vs. *number of cycles.* Concentration of dimer, $5 \cdot 10^{-3}$ M; concentration of $(Bu_4N)PF_6$, 0.1M; number of cycles, 10; scan rate, 0.01 $V \cdot s^{-1}$; potential range, from 0.00 to +1.15 V.

from the electrode surface. The increase of A_P observed in the first cycles of the voltabsorptometric experiment is in agreement with the necessity for the chain to reach a critical length to precipitate onto the electrode.

The oxidation of dimers proceeds faster on the polymer than on the Au surface, in such a way that the higher the amount of polymer film covering the electrode, the higher the amount of oxidized dimer and, consequently, the easier the attainment of the critical chain length suitable for precipitation onto the electrode (growing step). Both steps, with different polymer growth rates, have been observed under all experimental conditions.

The maximum oxidation potential reached in the voltammetric scan is an important experimental parameter affecting the amount of polymer and oligomers generated. *Fig. 6,a* shows the evolution of A_P at 400 nm and of A_N^C at 564 nm at 0.00 V *vs.* number of cycles during a ten-cycle voltabsorptometric experiment from 0.00 V to +1.12 V. *Fig. 6,b* shows the results of a similar experiment when the most anodic potential is + 1.08 V. Evolutions of A_N^C and A_P are qualitatively similar in both experiments: after the first cycles, in which a large amount of oligomers form, though very little polymer is detected, the polymer film starts increasing at a constant rate for each cycle, while the oligomer concentration remains practically unchanged. The main difference lies in the fact that, when the maximum potential in the oxidation scan is +1.08 V, five potential cycles are necessary to generate a high enough oligomer concentration to lead to quite a significant amount of polymer, whereas only one or two cycles are sufficient in the experiment, reaching the anodic limit of +1.12 V.

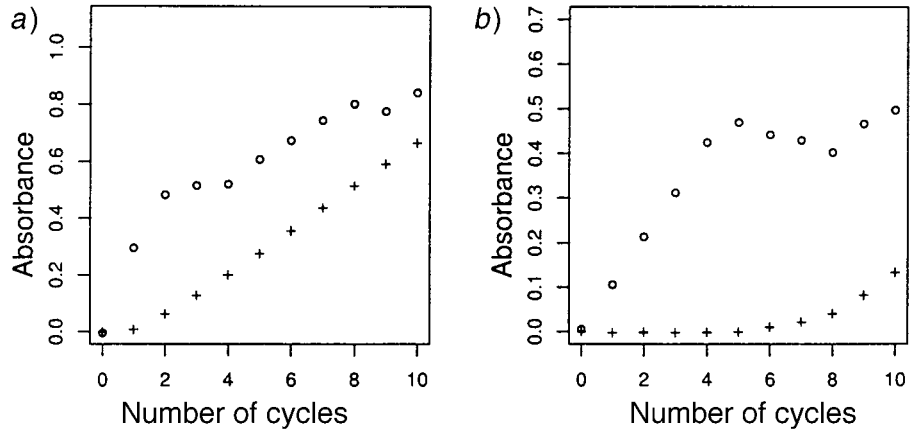

Fig. 6. *Evolution of* A_P (○) *at 400 nm and* A_N^C (+) *at 564 nm at 0.00 V* vs. *number of cycles: potential range* a) *from 0.00 to +1.12 V and* b) *from 0.00 to 1.08 V.* Concentration of dimer, $2 \cdot 10^{-3}$ M; concentration of $(Bu_4N)PF_6$, 0.1M; number of cycles, 10; scan rate, 0.02 $V \cdot s^{-1}$; diffusion space, 150 μm.

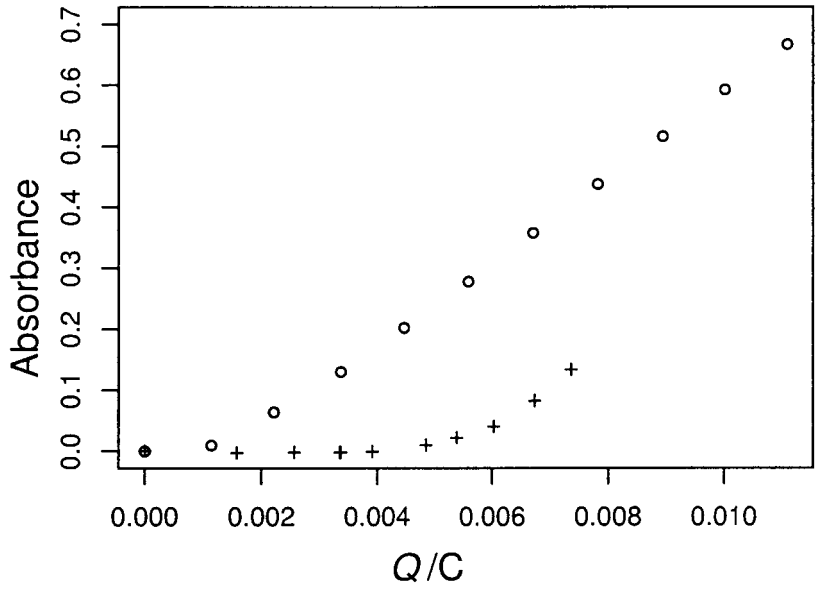

Fig. 7. *Absorbance in normal configuration,* A_N^C, *at 564 nm* vs. *electric charge,* Q, *at 0.00 V: potential range from 0.00 to +1.12 V* (○) *and from 0.00 to +1.08 V* (+). Experimental conditions as in *Fig. 6.*

Measurements of the electric charge, Q, support the results reported above. When measured at 0.00 V, Q increases linearly with the number of cycles in the two experiments described above. If the absorbance in normal configuration, A_N^C, at $\lambda = 564$ nm, is plotted against Q (*Fig. 7*), it is evident that, during the first cycles, most of the electric charge is not used in the formation of polymer but rather in the generation of oligomers. Once the polymer film starts forming, Q and A_N^C are linearly related to each other.

3.3. *Spectroelectrochemical Characterization of the Polymer.* As an example, characterization of the polymer obtained under the experimental conditions described in *Fig. 2* was carried out by voltabsorptometry in the thin-layer bidimensional arrangement. The polymer-coated electrode was dipped in a dimer-free MeCN solution containing only 0.1M $(Bu_4N)PF_6$ supporting electrolyte. The potential was scanned between 0.00 and +0.80 V at 0.02 $V \cdot s^{-1}$. *Fig. 8* reports a plot of the variations of absorbance, $\Delta A_N = |A_N - A_N^0|$ and $\Delta A_P = |A_P - A_P^0|$, at 564 nm, registered during ten subsequent cycles, against the electrode potential. ΔA_N increases when the polymer is oxidized, whereas ΔA_P assumes a constant value of zero. This means that no soluble species is released during the electro-oxidation of the polymer and also confirms that electrodeposited polymer does not interfere with the absorbance measurement in the parallel arrangement, as we have assumed at the beginning of our tests.

Figs. 9,a and *b* show the voltammogram and the derivative voltabsorptogram, respectively, obtained in normal configuration during the described characterization process. The signals are morphologically similar, the main difference being the presence of the capacitive component in the current signal. Ten subsequent potential scans are represented, the responses obtained being identical from the second scan onwards, which implies a high stability of the polymer film. As usual, the first cycle of the voltammogram is slightly different from the following ones, especially in the anodic scan. The same effect is found in the spectroscopic signal and is usually attributed to the 'memory effect'. Besides that, no difference between polaron and bipolaron formation responses can be evidenced.

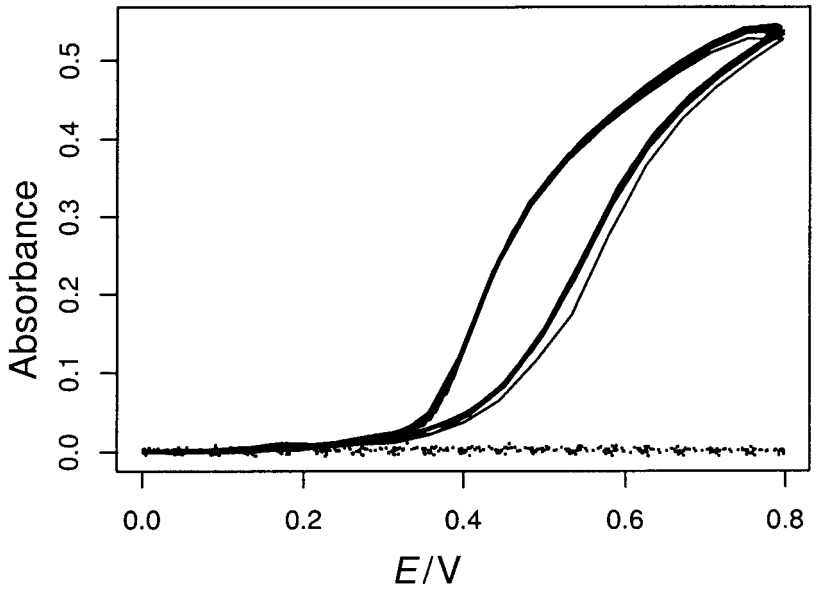

Fig. 8. *Plot of the variations of absorbance,* ΔA_N (solid line) *and* ΔA_P (dotted line) *at 564 nm* vs. *potential during the characterization of the polymer obtained under conditions presented in* Fig. 2. Concentration of $(Bu_4N)PF_6$, 0.1M; number of cycles, 10; scan rate, 0.02 $V \cdot s^{-1}$; potential range from 0.00 to +0.80 V; diffusion space, 150 μm.

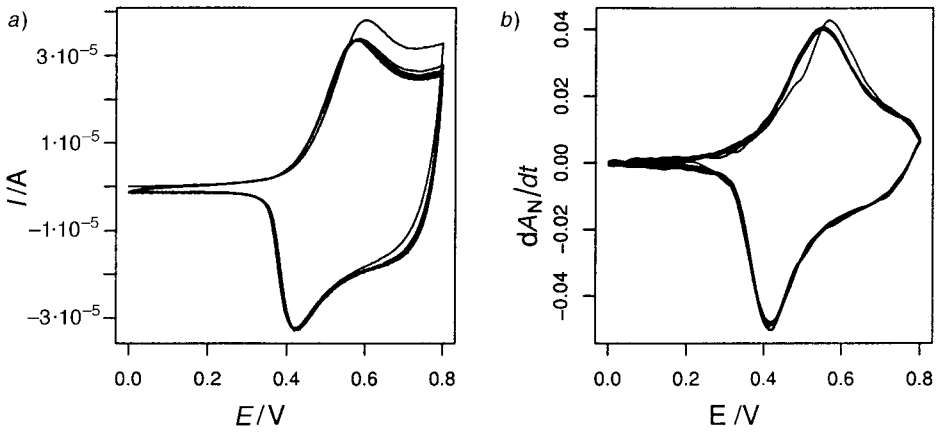

Fig. 9. a) *Cyclic voltammogram and* b) *derivative cyclic voltabsorptogram in normal configuration corresponding to the experience of* Fig. 2.

4. Conclusions. – Bidimensional absorbance measurements carried out during the electropolymerization of 4,4′-bis(butylthio)-2,2′-bithiophene (**1**) allow us to state that generation of polymer takes place in two steps, nucleation and growing, that differ in the rate at which the polymer appears on the electrode surface. The nucleation stage is characterized by a very low polymerization rate but, at the same time, by a high rate of oligomers generation. Actually, oligomeric species form continuously during the second step, when the polymer-growing rate increases considerably. Generation of oligomers can not be considered as a side reaction of the actual polymerization, but rather as a necessary step in both the nucleation and the polymer growth on the electrode. The maximum oxidation potential applied to the electrode in the potentiodynamic electropolymerization influences notably the rate of generation of short-chain oligomers and, consequently, the speed of the nucleation stage. No polymeric species diffuse into the solution. The polymer remains deposited onto the electrode and shows high electrochemical stability, no oligomeric soluble species being formed by repeated charging and discharging of the polymer coating.

Support of the *DGICYT* (PB93-0677) and *Junta de Castilla y León* (BU11/98) is gratefully acknowledged. The authors are grateful to Prof. *L. Schenetti*, Department of Chemistry, University of Modena, for supplying the 4,4′-bis(butylthio)-2,2′-bithiophene dimer.

Experimental Part

General. Solns. were prepared in MeCN, with $(Bu_4N)PF_6$ as supporting electrolyte. All chemicals were of *p.a.* quality and used without further purification.

Spectro- and Electrochemical Equipment. Voltabsorptometric experiments were carried out by means of a conventional three-electrode system controlled by a *PGSTAT 20* (*Eco Chemie B.V.*, The Netherlands) potentiostat. A light source *DH-2000* (*Top Sensor Systems*, The Netherlands) consisting of a double lamp, halogen and deuterium, and a modular system composed of two spectrometers and two diode-array detectors with 2048 elements (*S2000 Ocean Optics*, USA) were assembled by means of optic fibers, as previously described [39].

Spectroelectrochemical Cell. A special cell was designed and constructed in our laboratory [39], based on a planar optically transparent Au electrode allowing the light beams to cross the soln. simultaneously in both

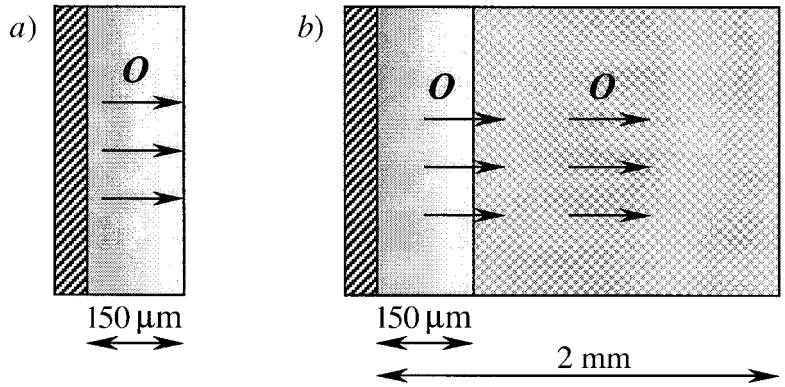

Fig. 10. *Cross-section of the spectroelectrochemical cells used for* a*) finite and* b*) semi-infinite diffusion conditions.* From left to right: Au electrode (stripped section), light sampled diffusion space (grey section); solution which does not contribute to A_P (dotted section).

normal and parallel directions to the electrode surface (*Fig. 1*). The Au film was sputtered (*Emitech K550*, UK) over a piece of glass or quartz of suitable dimensions. Small modifications were introduced on the original cell with the aim of making the device resistant to org. solvents. All the potentials were measured against a Ag/AgCl reference electrode.

Figs. 10,*a* and *b* show cross-sections of the cells used for finite and semi-infinite diffusion conditions, resp. In the former cell geometry, the diffusion space is limited to 150 µm and the light beam (parallel configuration) crosses the whole width of the space where the species is confined during electropolymerization. On the contrary, under semi-infinite-diffusion conditions (*Fig. 10*,*b*), a mask restricts the optical path length to the same value (150 µm), but the species formed at the electrode surface are allowed to diffuse beyond this distance, into the bulk of the soln. In this case, the light-beam section (parallel configuration) is smaller than the whole diffusion-layer thickness.

4,4′-Bis(butylthio)-2,2′-bithiophene (**1**). The dimer **1** was obtained from the corresponding dibromo derivative as reported previously [41]. All anal. characterizations of the dimer and of the relevant polymer were completely consistent with the data reported in [12][41].

REFERENCES

[1] G. Schopf, G. Kossmehl, *Adv. Polym. Sci*. **1997**, *129*, 143.
[2] H. S. Nalwa, ‘Handbook of Organic Conductive Molecules and Polymers’, Wiley, Chichester, 1997, Vol. 2.
[3] J. Roncali, *J. Mater. Chem*. **1999**, *9*, 1875.
[4] D. Fichou, ‘Handbook of Oligo- and Polythiophenes’, Wiley-VCH, Weinheim, 1999.
[5] D. T. McQuade, A. E. Pullen, T. M. Swager, *Chem. Rev.* **2000**, *100*, 2537.
[6] J. Heinze, ‘Topics in Current Chemistry’, Springer-Verlag, Berlin, 1990, Vol. 152.
[7] G. Inzelt, in ‘Electroanalytical Chemistry’, Ed. A. J. Bard, Marcel Dekker, New York, 1994, Vol. 18, p. 89.
[8] M. E. G. Lyons, ‘Electroactive Polymer Electrochemistry; Part 1, Fundamentals; Part 2, Methods and Applications’, Plenum Press, New York, 1994.
[9] H. B. Mark Jr., N. Atta, Y. L. Ma, K. L. Petticrew, H. Zimmer, Y. Shi, S. K. Lunsford, J. F. Rubinson, A. Galal, *Bioelectrochem. Bioenergetics* **1995**, *38*, 229.
[10] A. Malinauskas, *Synth. Met*. **1999**, *107*, 75.
[11] A. Smie, A. Synowczyk, J. Heinze, R. Alle, P. Tschuncky, G. Götz, P. Bäuerle, *J. Electroanal. Chem*. **1998**, *452*, 87.
[12] D. Iarossi, A. Mucci, L. Schenetti, R. Seeber, F. Goldoni, M. Affonte, F. Nava, *Macromolecules* **1999**, *32*, 1390.
[13] B. Ballarin, F. Costanzo, F. Mori, A. Mucci, L. Pigani, L. Schenetti, R. Seeber, D. Tonelli, C. Zanardi, *Electrochim. Acta* **2001**, *46*, 881.

[14] D. Iarossi, A. Mucci, F. Parenti, L. Schenetti, R. Seeber, C. Zanardi, A. Forni, M. Tonelli, *Chem.–Eur. J.* **2001**, *7*, 676.
[15] H. Ding, L. Pigani, R. Seeber, C. Zanardi, *J. New Mat. Electrochem. Systems* **2000**, *3*, 339.
[16] H. Ding, Z. Pan, L. Pigani, R. Seeber, C. Zanardi, *Electrochim. Acta* **2001**, *46*, 2721.
[17] H. Ding, Z. Pan, L. Pigani, R. Seeber, *J. New Mat. Electrochem. Systems* **2001**, *4*, 63.
[18] M. Belletête, L. Mazerolle, N. Sesrosiers, M. Leclerc, G. Durocher, *Macromolecules* **1995**, *28*, 8587.
[19] M. Lapkowski, A. Pron, *Synth. Met*. **2000**, *110*, 79.
[20] G. Shopf, G. Kossmehl, 'Polythiophenes – Electrically Conductive Polymers', Springer, Germany, 1997.
[21] M. Skompska, *Electrochim. Acta* **1998**, *44*, 357.
[22] X. Hu, G. Wang, T. K. S. Wong, *Synth. Met*. **1999**, *106*, 145.
[23] H. P. Welzel, G. Kossmehl, G. Engelmann, W. D. Hunnius, W. Plieth, *Electrochim. Acta* **1999**, *44*, 1827.
[24] C. Visy, J. Kankare, E. Kriván, *Electrochim. Acta* **2000**, *45*, 3851.
[25] I. Villareal, E. Morales, J. L. Acosta, *Polymer* **2001**, *42*, 3779.
[26] J. Heinze, H. John, M. Dietrich, P. Tschuncky, *Synth. Met*. **2001**, *119*, 49.
[27] J. Heinze, in 'Organic Electrochemistry', Eds. H. Lund and O. Hammerich, Marcel Dekker, New York, 2001.
[28] E. Genies, G. Bidan, A. F. Díaz, *J. Electroanal. Chem*. **1983**, *149*, 113.
[29] J. Roncali, *Chem. Rev*. **1992**, *92*, 711.
[30] A. R. Hillman, E. F. Mallen, *J. Electroanal. Chem*. **1987**, *220*, 351.
[31] A. R. Hillman, E. F. Mallen, A. Hamnett, *J. Electroanal. Chem*. **1988**, *244*, 353.
[32] A. R. Hillman, M. J. Swann, *Electrochim. Acta* **1988**, *33*, 1303.
[33] K. Tanaka, T. Shichiri, S. Wang, T. Yamabe, *Synth. Met*. **1988**, *24*, 203.
[34] S. Asavapiriyanont, G. K. Chandler, G. A. Gunawardena, D. Pletcher, *J. Electroanal. Chem.* **1984**, *177*, 229.
[35] R. John, G. G. Wallace, *J. Electroanal. Chem*. **1991**, *306*, 157.
[36] G. Casalbore-Miceli, N. Camaioni, A. Geri, M. Cristani, A. M. Fichera, A. Berlin, *Synth. Met*. **2000**, *108*, 47.
[37] A. F. Diaz, J. L. Castillo, J. A. Logan, W. Y. Lee, *J. Electroanal. Chem*. **1982**, *129*, 115.
[38] M. Olbrich-Stock, J. Posdorfer, R. N. Schindler, *J. Electroanal. Chem*. **1994**, *368*, 173.
[39] J. López-Palacios, A. Colina, A. Heras, V. Ruiz, L. Fuente, *Anal. Chem*. **2001**, *73*, 2883.
[40] Q. Xie, W. Wei, L. Nie, S. Yao, *Anal. Chem*. **1993**, *65*, 1888.
[41] U. Folli, F. Goldoni, D. Iarossi, A. Mucci, L. Schenetti, *J. Chem. Res.* **1996**, 69.

Received May 30, 2001